# Atomic background in x-ray absorption spectra of fifth-period elements: Evidence for double-electron excitation edges

Adriano Filipponi
*Dipartimento di Fisica, Università degli Studi dell' Aquila, Via Vetoio, 67010 Coppito, L'Aquila, Italy*

Andrea Di Cicco
*Dipartimento di Matematica e Fisica, Università degli Studi di Camerino, Via Madonna delle Carceri, 62032 Camerino (MC), Italy*
(Received 14 February 1995)

A systematic x-ray absorption study to detect atomic background features at the $K$ edges of fifth-period elements is reported. Samples of $MoC_x$ ($Z = 42$) and pure Rh ($Z = 45$), Pd ($Z = 46$), Ag ($Z = 47$), In ($Z = 49$), and Sn ($Z = 50$) are measured at high temperature, mostly in the liquid phase, to reduce the intensity of the structural extended x-ray absorption fine structure (EXAFS) contribution. Main anomalies, showing a regular trend as a function of $Z$, are identified in the region around 100 eV and in the range 200–800 eV above an edge. They are assigned to the opening of absorption channels creating double-hole configurations such as $[1s4p]$, $[1s, 3d]$, and $[1s3p]$. Differences of self-consistent calculations in the Dirac-Fock approximation have been performed and the dominant transitions unambiguously identified. The results are relevant for the improvement of the EXAFS analysis at these edges.

PACS number(s): 32.30.Rj, 78.70.Dm, 32.80.Fb

## I. INTRODUCTION

Recent advances in the understanding of the fine structure of the x-ray absorption cross section above inner-shell excitation thresholds have stimulated fundamental research on the nature of the absorption background associated with isolated atoms. This background is directly accessible to experimental detection only in the case of noble gases and possibly high-vapor-pressure elements. More usually atoms are found bonded into molecules or condensed matter and the study of the atomic cross-section properties is hampered.

There are both fundamental and applicative aspects involved in this research. The atomic background is expected to contain features associated with the many-body relaxation of the atomic charge stimulated by the photon absorption. In a one-electron picture these phenomena can be represented by the creation of additional core holes. As an example, strong effects associated with the creation of simultaneous $K$ and $M$ holes are well known to occur in Ar and have been the subject of several accurate studies [1–3]. This phenomenology is also epitomized by the Kr case, well studied from both the experimental and theoretical points of view [4–6]. In Kr the onset of double-electron excitation channels above the $K$ edge, due to the formation of $[1s4p]$, $[1s4s]$, $[1s3d]$, and $[1s3p]$ double-core-hole configurations has been clearly identified. The excited electrons can be promoted to either discrete or continuum levels. Transitions to discrete autoionizing states can occur at the channel onsets (a wide phenomenology exists for the $KL$ edge of third-period elements [7]). Shake-up channels are given by transitions in which one electron is promoted to a discrete excited state and the other ejected. Shake-up channels contribute to the absorption continuum and can be identified by the corresponding photoelectron peaks in x-ray photoemission spectroscopy also in the case of additional core excitation [8]. Finally, if both electrons are excited to continuum levels a shake-off process is obtained. These phenomena also contribute to the absorption background but produce rather smooth effects, since the energy phase space, and roughly the cross section at threshold, increase linearly with energy. A recent study on $L$ edges of Xe [9] has brought novel insight into a rather complex absorption pattern in which all of these excitation mechanisms are involved.

These phenomena are relatively well known in the atomic physics context but they have rarely been considered for their practical consequences in the analysis of extended x-ray absorption fine structure (EXAFS) spectra. In a series of recent papers several groups have emphasized the importance of accounting for double-electron features of the atomic background to improve the EXAFS data analysis [10–12]. The picture that emerges from these investigations is that double-electron excitation effects are a rather general phenomenon and their presence is the rule rather than the exception.

Following a series of investigations by our group we have undertaken extensive research on the atomic background effects occurring above $K$ edges of fifth-period atoms. The results, involving experimental data on six different elements from Mo ($Z$=42) to Sn ($Z$=50), are presented in this paper.

The paper is organized as follows. In Sec. II the effects of the conventional background subtraction on the EXAFS analysis of solid Ag at room temperature are discussed. In Sec. III experimental details on samples and measurements are illustrated. The available exper-

 

imental data are reported and the double-electron excitation feature identified. Section IV presents the results of self-consistent relativistic atomic energy calculations. The final unambiguous assignments and the relevance for EXAFS data analysis are discussed in Sec. V. Section VI is devoted to the conclusions.

## II. THE Ag $K$-EDGE BACKGROUND

In the usual EXAFS analysis the structural oscillation is extracted from the raw absorption data by subtracting a background function modeled as a smooth polynomial spline. The spline is defined by the energy intervals in which the polynomial functions are matched for continuity and derivability and by the degree of each polynomial function. For a typical spectrum recorded at $K$ edges of fifth-period elements, where the signal extends more than 1000 eV above the edge, the number of spline coefficients is usually in the range 6–9. A typical extraction of the Ag $K$ edge $\chi(k)$ spectrum at room temperature (RT) is shown in Fig. 1. Slightly different $\chi(k)$ can be obtained according to the spline fitting prescription. It is common use in EXAFS analysis to repeat and try to improve the extraction until the $\chi(k)$ shows a regular oscillation. The typical pattern of the magnitude of the Fourier transform (FT) of the $\chi(k)$ signal calculated in the $k$ range 2.5–18 Å$^{-1}$ with a $k^2$ weight is reported in Fig. 2. In this picture the dominant component due to the Ag-Ag first-shell bond, peaking at $R \sim 2.6$ Å (not corrected for phase shift), is evident. Some weak contributions associated with more distant shells are also seen at larger distances. Surprisingly, weak ripples (arrow in Fig. 2) are also visible in the low-$R$ range, where physical interatomic distances are not occurring. These features are clearly associated with background effects and are not completely accounted for by the polynomial spline. It is well known that a change of the background spline affects the Fourier transform plot mainly in this low-$R$ region. As a matter of fact the adoption of a polynomial spline background is not sufficient to suppress these low-$R$ features in the FT. It is possible to reduce their intensity,

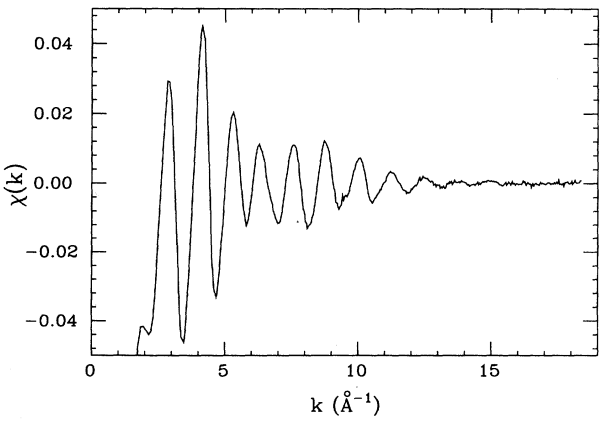


FIG. 1. EXAFS spectrum of microcrystalline Ag at RT extracted with a conventional spline function.

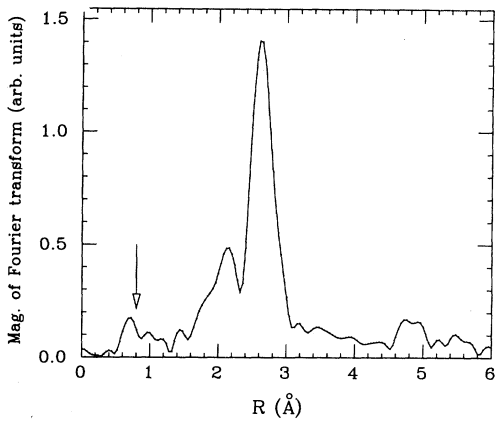


FIG. 2. Magnitude of the Fourier transform of the spectrum of Fig. 1 in the range $k = 2.5$–18 Å$^{-1}$ with a $k^2$ weight. The arrow indicates low-$R$ signal not associated with structural effects.

but is very hard to eliminate them unless a very flexible spline is used, or the useful EXAFS region reduced.

Within the current interpretation, low-$R$ features without structural meaning in the FT can be associated with the existence of background anomalies due to multielectron excitation effects [10–12]. The absence of any previous study on fifth-period elements stimulated us to undertake a detailed investigation on the subject.

## III. EXPERIMENTAL DETAILS

### A. High-temperature spectra

The aim of this experiment was to collect x-ray absorption spectra at the $K$ edge of several fifth-period elements under controlled experimental conditions such that the amplitude of the structural contribution was strongly reduced. In all cases the low vapor pressure of the elements and the nonexistence of volatile compounds binding low-$Z$ elements hampered us in performing gas phase experiments. An alternative strategy was to perform measurements under high-temperature conditions in order to produce a large thermal damping of the structural contributions due to the Debye-Waller effect. This is similar to what was performed in a previous investigation on $L$ edges of sixth-period elements [13]. In the present case we took advantage of a new high-temperature EXAFS technique, previously developed by us [14], that allows one to perform EXAFS measurements on low-vapor-pressure condensed matter up to the 3000 K temperature range.

The experimental spectra reported in this paper have been collected during dedicated beamtime at Laboratoire pour l'Utilisation du Rayonnement Electromagnétique (Orsay, Paris, France) at the D44-EXAFS4 beamline equipped with a double-crystal Si (311) monochromator. Ion chambers were filled with Kr gas to minimize the noise in the absorption detection. The DCI storage ring was operating at 1.85 GeV with currents in the 300 mA range. The beamline was equipped with the high-temperature oven previously described [14].

The Mo $K$-edge study was performed on molybdenum

carbide powder $MoC_x$, whereas samples for the Rh, Pd, Ag, In, and Sn $K$ edges were made of the pure elements in microcrystalline form. The measurements were performed, in all cases, above the respective metal melting points $T_m$ to obtain a drastic reduction of the intensity of the EXAFS signal due to the disorder in the liquid phase. In particular, the measurement temperatures were respectively $\sim$ 2800 K for $MoC_x$, 2300 K for Rh, 1850 K for Pd, 1250 K for Ag, 1170 K for In, and 1400 K for Sn. The temperatures for In and Sn were well above the respective $T_m$.

The energy calibration was performed by setting selected features of reference metallic foil spectra to the corresponding tabulated values [15]. The energy resolution of the spectra was found to be in the range of a few eV rising from about 5 eV for Mo to about 7 eV for Sn. The resulting broadening of the features, however, is found to be effective only in the edge region; the intrinsic widths of the double-electron excitation features are, for these edges, much broader than the resolution limit.

### B. Reduction of EXAFS amplitude

The effect of the reduction of the EXAFS amplitude from RT to the molten species is shown for the case of Ag. The raw absorption spectra for crystalline Ag at 300 K (RT) and molten Ag at 1250 K are reported in Fig. 3. The relevant features of the spectra are better evidenced in a magnified plot reporting the dimensionless, normalized, absorption excess $\Delta\alpha$ as a function of the energy distance above threshold $E_t$. The threshold energy is defined by the inflection point of the absorption. $\Delta\alpha$ is defined as the absorption background excess with respect to a linear average decay, fitted in the EXAFS region, and is normalized to the main $K$-edge discontinuity. We point out that absolute cross sections can hardly be obtained from our data due to the unknown sample quantity and the presence of an inert material in which the sample is dispersed. For this reason mostly relative quantities with respect to the main $K$-edge absorption discontinuity are reported. Tabulated cross-section values can be used for an absolute calibration of the $\Delta\alpha$ scale with an accuracy of about 5%.

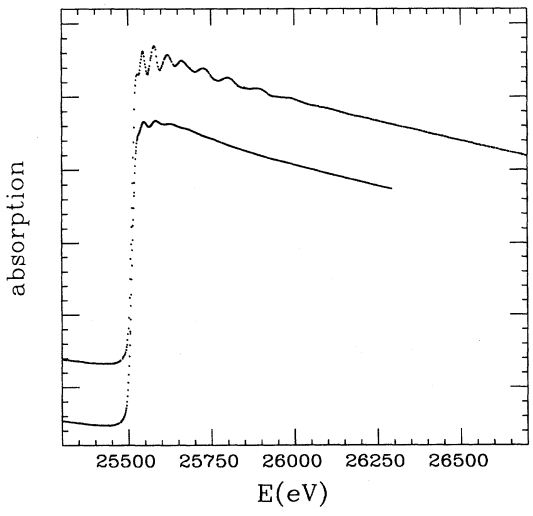


FIG. 3. Raw absorption Ag $K$-edge spectra for microcrystalline Ag at RT (upper spectrum) and liquid Ag at 1250 K.

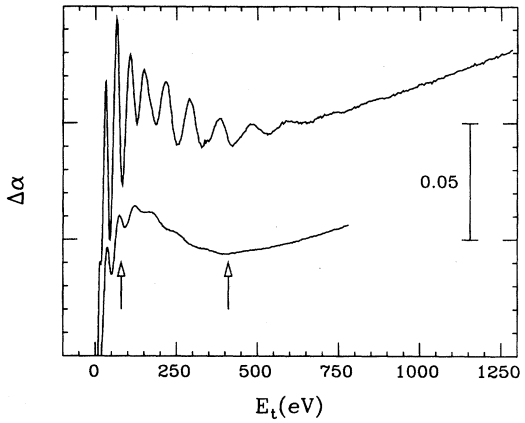


FIG. 4. Absorption excess $\Delta\alpha$ with respect to a linear decay at the Ag $K$ edge as a function of the energy above threshold $E_t$; microcrystalline Ag at RT (upper spectrum), liquid Ag at 1250 K (lower spectrum). The underlying atomic background is similar. Arrows indicate the main background anomalies.

In Fig. 4 the top spectrum refers to crystalline Ag at 300 K (RT) and the bottom spectrum to molten Ag at 1250 K. The intensity of the EXAFS is strongly reduced and possible anomalies in the background are evidenced. Looking at the bottom spectrum in Fig. 4 it appears that the underlying background is quite complex. In addition to the weak residual structural oscillation there are at least two features (indicated by the arrows) associated with noticeable slope changes clearly visible on these raw data. We point out that the same underlying background is present in both RT and high-temperature data. Other experiments on different compounds reveal that this background is also present there with similar shapes; in practice it is realized that the profile shown by these spectra is characteristic of the Ag atomic background. It is exactly this profile that can hardly be accounted for by the adoption of a polynomial spline.

### C. Spectra of fifth-period elements

The raw data for the other elements and compounds have been treated similarly to the Ag spectra in Fig. 4 and the corresponding $\Delta\alpha(E_t)$ spectra are reported in Fig. 5. The spectra are normalized to the respective $K$-edge discontinuities and are offset vertically by 0.02 units for clarity; the $E_t$ scale instead is the same, referring to each respective threshold. The spectra are ordered from top to bottom in ascending atomic number. Notice that there is a gap of two elements between Mo and Rh and of one element between Ag and In. In all cases a considerable reduction of the EXAFS intensity with respect to the corresponding room temperature spectra is obtained. The most spectacular feature revealed by this comparison

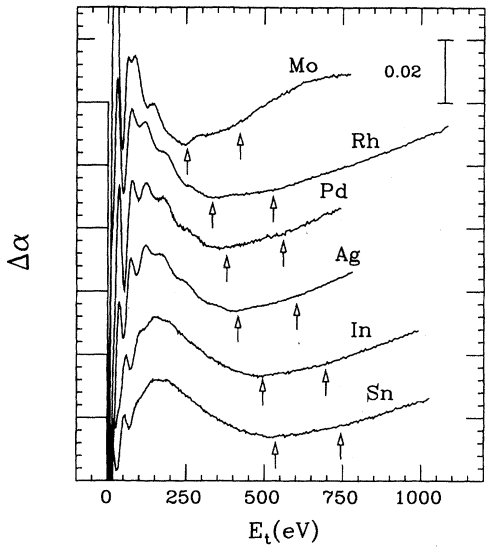


FIG. 5. Absorption $K$-edge excess $\Delta\alpha$ as a function of the energy above the respective thresholds $E_t$ in $MoC_x$ at $\sim$ 2800 K, and liquid Rh at 2300 K, Pd at 1850 K, Ag at 1250 K, In at 1170 K, and Sn at 1400 K. Notice the regular trend in the background features as a function of $Z$. Vertical arrows refer to theoretical calculations of the thresholds for shake-up channels involving the additional excitation of $3d_{5/2}$ and $3p_{3/2}$ electrons, respectively (see text).

is the clear trend in the background versus $Z$. For example, the evident slope change occurring in Ag around $E_t \sim 380$ eV shifts from Mo at $E_t \sim 250$ eV to Sn at $E_t \sim 520$ eV. A similar trend is shown by the features closer to the $K$ edge magnified in Fig. 6 where a clear absorption step of 0.02–0.03 units, visible in Mo, Rh, Pd,

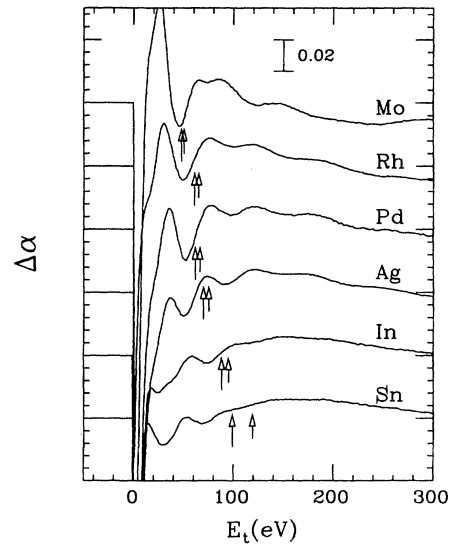


FIG. 6. $\Delta\alpha(E_t)$ for $MoC_x$ at $\sim$ 2800 K, liquid Rh at 2300 K, Pd at 1850 K, Ag at 1250 K, In at 1170 K, and Sn at 1400 K, in the 0–300 eV energy region. Vertical arrows refer to theoretical calculations of the thresholds for shake-up channels involving the additional excitation of $4p_{3/2}$ and $4p_{1/2}$ (shorter arrow) electrons, respectively.

and Ag, gradually shifts to higher energies.

This phenomenology is an unambiguous signature for atomic background effects associated with the internal electronic structure. Shallow core electrons have binding energies comparable with the observed features. In particular, $3d_{5/2}$ electrons have a binding energy ranging from ~228 eV for Mo to $\sim$ 485 eV for Sn and their additional excitation is to be associated with the main slope change in the central region of the spectra. Similarly, the additional excitation of $4p$ electrons is to be associated with the low-energy absorption increase. A more precise comparison with theoretically predicted energy onsets for double-electron excitation channels will be performed in the next section.

In order to make a more precise identification of the experimental background features in the high-energy part of the spectra, we calculated the derivatives $d\alpha/dE(E_t)$ averaging the slope over intervals of 16 points of the original spectra. The results are reported in Fig. 7 in the range $E_t = 200 - 1000$ eV. The slope changes assigned to the $3d$ excitations are clearly visible as isolated steps in the $d\alpha/dE(E_t)$ spectra. A weaker second slope change, associated with the additional excitation of $3p$ electrons, is also detected at higher energies. In both cases a regular trend versus $Z$ is observed.

A careful analysis of Fig. 7 reveals the presence of a weak slope change in the region between the $[1s3d]$ and $[1s3p]$ onsets, that is mainly visible in Ag, In, and Sn (dashed line). A possible assignment is the threshold for triple-electron excitations $[1s3d4p]$ that should occur in this energy region. This excitation was previously observed by Ito and co-workers at the Kr [5] and Br [16] $K$ edges.

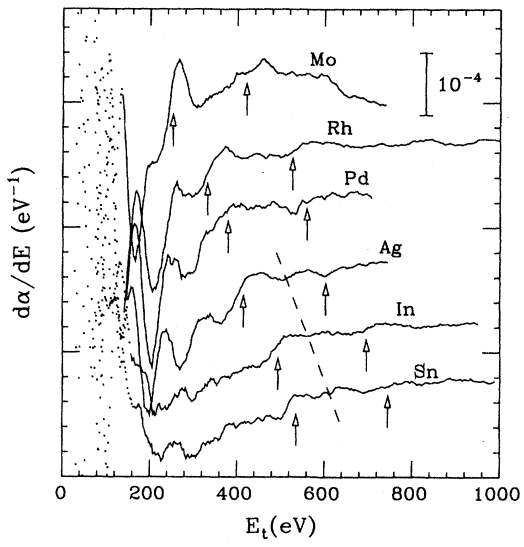


FIG. 7. Derivative $d\alpha/dE$ as a function of the energy above the respective thresholds $E_t$ in $MoC_x$ at $\sim$ 2800 K, and liquid Rh at 2300 K, Pd at 1850 K, Ag at 1250 K, In at 1170 K, and Sn at 1400 K. The discontinuities are associated with the slope changes in the absorption coefficient. Vertical arrows refer to the $3d_{5/2}$ and $3p_{3/2}$ theoretical shake-up thresholds. The dashed line interpolates the position of a further slope change tentatively assigned to the $[1s3d4p]$ excitations.

TABLE I. Estimates of the positions of the slope discontinuities in the experimental spectra, due to the transitions creating $[1s3d]$, $[1s3d4p]$ (tentative assignment), and $[1s3p]$ core-hole configurations. For Mo $[1s3d]$ the value refers to the absorption discontinuity $\Delta\alpha$.

| | | $[1s3d]$ | | $[1s3d4p]$ | | $[1s3p]$ | |
|---|---|---|---|---|---|---|---|
| $Z$ | Symbol | $E_t$ (eV) | $\Delta\alpha'$ ($10^{-5}$ eV$^{-1}$) | $E_t$ (eV) | $\Delta\alpha'$ ($10^{-5}$eV$^{-1}$) | $E_t$ (eV) | $\Delta\alpha'$ ($10^{-5}$eV$^{-1}$) |
| 42 | Mo | 250(10) | [$\Delta\alpha$ 0.005(1)] | | | 430(10) | |
| 45 | Rh | 340(10) | 7(2) | | | 520(20) | 3(1) |
| 46 | Pd | 350(20) | 9(3) | | | 540(20) | 2(1) |
| 47 | Ag | 410(15) | 8(2) | 520(20) | 2(1) | 610(20) | 2(1) |
| 49 | In | 480(20) | 7(2) | 570(20) | 1(1) | 680(20) | 2(1) |
| 50 | Sn | 520(20) | 5(1) | 600(20) | 1.5(5) | 720(20) | 1(1) |

In Table I we summarize the energy positions on the $E_t$ scale and the observed slope changes $\Delta\alpha'$ of these high-energy experimental features.

## IV. CALCULATION OF EXCITATION ENERGIES

In order to make a precise assignment and to confirm the suspected origin of the observed background anomalies we made a calculation of the excitation energies required to create additional core holes in the atom. Total energy calculations were performed using a relativistic atomic self-consistent scheme [17]. Excitation energies can be estimated by the difference between the atomic ground state and the excited state energies, with an accuracy of about 0.3% in the present cases. A convenient and accurate way to locate the features is the calculation of difference of excitation energies between the main $K$-edge channel and the double-electron excitation threshold. In the present case we adopted as a reference energy that of the ionized atom with a $[1s]$ core hole, corresponding to the continuum threshold of the $K$-edge channels. Notice that this level is located a few eV above the inflection point at the $K$ edge used as a zero for the $E_t$ scale. The energies for the onsets of the double-excitation channels were calculated starting from shake-up configurations of the type $[1snl_j]ml_j$, where the additional electron has been promoted from the $n$ level to the first unfilled level ($m$) with the same $l$ and $j$ quantum numbers. The difference between the total energies of the atom in these two configurations provides an estimate of the lowest extra energy required to excite the second electron in the presence of the main core hole. It should be noted that there is usually a spread of several tens of eV from the lowest discrete excitations to the shake-off threshold (typically located 5–20 eV above the lowest shake-up channel, in these cases). Multiplet splitting produces a further broadening of the double-electron excitation threshold. Therefore it is not obvious where the theoretical onset for observable excess cross section is actually located and the agreement between theoretical estimates and experimental positions should be analyzed at the level of $\pm 20$ eV.

The calculated difference energies for the various excitation channels are reported in Table II according to the following scheme: $\Delta E(4p_{3/2}) = E([1s4p_{3/2}]mp_{3/2}) - E([1s])$, $\Delta E(4p_{1/2}) = E([1s4p_{1/2}]mp_{1/2}) - E([1s])$, $\Delta E(3d_{5/2}) = E([1s3d_{5/2}]md_{5/2}) - E([1s])$, $\Delta E(3d_{3/2}) = E([1s3d_{3/2}]md_{3/2}) - E([1s])$, $\Delta E(3d_{5/2}4p_{3/2}) = E([1s3d_{5/2}4p_{3/2}]md_{5/2}m'p_{3/2}) - E([1s])$, $\Delta E(3p_{3/2}) = E([1s3p_{3/2}]mp_{3/2}) - E([1s])$, $\Delta E(3p_{1/2}) = E([1s3p_{1/2}]mp_{1/2}) - E([1s])$. The $m$ level is usually $m = n + 1$. When the $n + 1$ level is already filled in the ground state configuration the electron is placed in the corresponding $n + 2$ level. For $p_{3/2}$ electrons this occurs from $Z = 54$, for $p_{1/2}$ electrons from $Z = 50$, for $d_{5/2}$ electrons from $Z = 46$, and for $d_{3/2}$ electrons from $Z = 44$.

The predicted energies for $\Delta E(3d_{5/2})$ and $\Delta E(3p_{3/2})$ are indicated as small vertical arrows in Fig. 5 and Fig. 7, and those of $\Delta E(4p_{3/2})$ and $\Delta E(4p_{1/2})$ are indicated in Fig. 6.

TABLE II. Differences of total energy calculations between excited shake-up states and the $K$-edge continuum threshold based on Dirac-Fock total energy calculations.

| | $\Delta E$ (eV) | | | | | | |
|---|---|---|---|---|---|---|---|
| $Z$ | $4p_{3/2}$ | $4p_{1/2}$ | $3d_{5/2}$ | $3d_{3/2}$ | $3d_{5/2}4p_{3/2}$ | $3p_{3/2}$ | $3p_{1/2}$ |
| 37 | 26.3 | 27.4 | 136.7 | 138.5 | 166.7 | 264.3 | 274.5 |
| 38 | 32.6 | 33.9 | 159.4 | 161.5 | 195.8 | 296.4 | 308.0 |
| 39 | 37.1 | 38.8 | 181.7 | 184.1 | 222.5 | 327.0 | 340.3 |
| 40 | 41.6 | 43.5 | 204.8 | 207.6 | 250.0 | 358.5 | 373.6 |
| 41 | 43.4 | 45.7 | 227.4 | 230.5 | 274.0 | 387.4 | 404.5 |
| 42 | 47.7 | 50.4 | 252.3 | 255.9 | 303.2 | 420.8 | 440.1 |
| 43 | 55.0 | 58.2 | 279.6 | 283.7 | 338.1 | 459.2 | 480.8 |
| 44 | 56.3 | 60.0 | 304.9 | 329.4 | 364.3 | 490.6 | 514.8 |
| 45 | 60.7 | 64.9 | 332.6 | 359.3 | 396.4 | 527.0 | 554.1 |
| 46 | 61.7 | 66.4 | 378.9 | 385.2 | 448.7 | 560.4 | 590.6 |
| 47 | 69.6 | 75.0 | 414.9 | 422.1 | 493.3 | 603.3 | 636.8 |
| 48 | 78.2 | 84.3 | 452.8 | 460.8 | 540.4 | 648.1 | 685.2 |
| 49 | 88.1 | 95.0 | 493.7 | 502.5 | 591.6 | 695.6 | 736.5 |
| 50 | 98.6 | 118.8 | 536.2 | 546.1 | 645.2 | 745.0 | 802.6 |
| 51 | 109.8 | 132.6 | 580.8 | 591.7 | 701.4 | 796.4 | 860.1 |
| 52 | 121.6 | 147.2 | 627.1 | 639.1 | 759.9 | 849.6 | 920.0 |
| 53 | 133.9 | 162.4 | 675.2 | 688.5 | 820.7 | 904.7 | 982.0 |
| 54 | 164.6 | 178.2 | 725.0 | 739.6 | 904.6 | 979.7 | 1046.3 |

## V. DISCUSSION

Prediction of channel intensities is out of the scope of the present report; notice, however, that the channel with higher $j$ (for the same $l$) is expected to have a larger weight in the process.

By comparing the calculated excitation energies in Table II with the experimental background profiles in Fig. 5, Fig. 6, and Fig. 7, the assignment of the main features is confirmed. The background anomaly around $E_t = 100$ eV is clearly associated with the shake channels involving $4p$ electrons. The presence of the residual EXAFS does not allow the identification of precise features. However, the observed trend from a rather sharp absorption step visible in Mo, Rh, Pd, and partly Ag to a rounded maximum in In and Sn is to be associated with the increasing binding energy of the $4p$ electrons and the gradual filling of the $5p$ levels in In and Sn.

The assignment of the main slope change in the central energy region of the spectra is consistent with the calculation of $\Delta E(3d_{5/2})$ and $\Delta E(3d_{3/2})$. The experimental feature becomes smoother as $Z$ is increased. Notice that, due to the progressive filling of the $4d$ orbitals from Mo to Ag, the intensity of the strongest shake-up $3d \rightarrow 4d$ is expected to decrease progressively. Consequently in In and Sn only weak shake-up contributions to higher discrete levels and shake-off contributions are expected. This occurrence suggests that the underlying slope change is mainly due to the opening of shake-off channels, whereas effects from shake-up channels might be visible in the lower-$Z$ cases.

The weaker slope change at higher energies is in excellent agreement with the predicted position of the onsets of $3p$ excitations. In this case shake-off channels should dominate since the $4p$ levels are occupied.

Finally, the predicted energy positions of the $[1s3d4p]$ excitations are in good agreement with the observed weak discontinuities intermediate between $[1s3d]$ and $[1s3p]$.

In general the theoretical excitation energies are found to be in perfect agreement with experimental determinations. They are quite helpful in the unambiguous assignment of the features. It should be recalled that uncertainty in the experimental values amounts to about $\pm 20$ eV, and that the energy calculations are based on an atomic scheme and multiplet splitting is neglected.

The relevance of the present findings for EXAFS data analysis is remarkable. We have shown that the $K$ edges of Mo, Rh, Pd, Ag, In, and Sn (but similar effects are expected for all fifth-period elements) are affected by the presence of atomic background anomalies due to double-electron excitation thresholds. These features, which are commonly ignored, should instead be taken into account for a correct EXAFS extraction, especially in those cases where the structural signal is weak. As is obvious from Fig. 5 their account is essential in the case of liquid systems. A flexible polynomial spline can be used especially for the high-$Z$ elements; however, this procedure introduces a large arbitrariness in the analysis and decreases the accuracy in the extracted structural parameters.

We attempted to model the atomic background of the $K$-edge spectra under consideration with a low-order polynomial spline plus specific double-electron contributions introduced using previously proposed empirical shapes. In particular, we were able to model the absorption step due to the $4p$ excitations with a three-parameter function previously proposed for Si $KL$ edges [10] and the slope discontinuity due to the $3d$ excitations with a model function used in the Br case [11] with the parameter $H = 0$. The Fourier transform spectra did not show the ripples in the low-$R$ range obtained using a smooth polynomial atomic background (see Fig. 2). In all cases the fitting discontinuity was comparable with the values obtained in the graphical analysis reported in Table II.

## VI. CONCLUSION

In the present paper a detailed investigation of the underlying atomic background at the $K$ edges of fifth-period elements has been reported. Six different elements ranging from Mo ($Z = 42$) to Sn ($Z = 50$) were considered. The paper addresses the problem of the correct account of the nonstructural background in EXAFS analysis at these $K$ edges for pure elements and their compounds, all having wide applicative interest. The main results of this research can be summarized as follows.

(1) Additional excitations of $4p$ electrons giving rise to secondary absorption steps of 2–3 % have been detected, especially in the lowest-$Z$ cases.

(2) A main slope change in the middle of the EXAFS range [amounting to $(5-9)\times 10^{-5}$ eV$^{-1}$] associated with additional excitations of $3d$ electrons is clearly identified.

(3) A weaker slope change associated with additional excitations of $3p$ electrons is also seen in all spectra.

(4) Another slope change is observed in Ag, In, and Sn, between the $3d$ and $3p$ features. It has been tentatively assigned to a triple-electron excitation involving $3d$ and $4p$ additional electrons.

(5) Total energy Dirac-Fock calculations have been performed for all fifth-period elements and the threshold energies for multielectron excitation channels with respect to the $K$-edge continuum threshold have been estimated by means of total energy differences. Good agreement is found with the position of the experimental features and the assignments are confirmed.

(6) The double-electron excitation effects discussed in the points (1) and (2) above are relatively strong and their account, for example, using appropriate empirical functions, is strongly recommended to perform a reliable EXAFS analysis at these edges.

## ACKNOWLEDGMENTS

We would like to thank the LURE staff, and in particular F. Villain and D. Bazin for technical assistance during the experiment. We would also like to thank M. Minicucci and F. Sperandini for their help in the preparation of the experiment. Part of this research has been financed through the Consiglio Nazionale delle Ricerce, contributo di ricerca No. 93.01301.CT02.

[1] H. W. Schnopper, Phys. Rev. **131**, 2558 (1963).
[2] R. D. Deslattes, R. E. LaVilla, P. L. Cowan, and A. Henins, Phys. Rev. A **27**, 923 (1983).
[3] M. Deutsch, N. Maskil, and W. Drube, Phys. Rev. A **46**, 3963 (1992).
[4] M. Deutsch and M. Hart, Phys. Rev. A **34**, 5168 (1986); E. Bernieri and E. Burattini, *ibid.* **35**, 3322 (1987).
[5] Y. Ito, H. Nakamatsu, T. Mukoyama, K. Omote, S. Yoshikado, M. Takahashi, and S. Emura, Phys. Rev. A **46**, 6083 (1992).
[6] S. J. Schaphorst, A. F. Kodre, J. Ruscheinski, B. Crasemann, T. Åberg, J. Tulkki, M. H. Chen, Y. Azuma, and G. S. Brown, Phys. Rev. A **47**, 1953 (1993).
[7] A. Filipponi, T. A. Tyson, K. O. Hodgson, and S. Mobilio, Phys. Rev. A **48**, 1328 (1993).
[8] N. Mårtensson, S. Svensson, and U. Gelius, J. Phys. B **20**, 6243 (1987); A. Filipponi, S. Di Nardo, M. Passacantando, L. Lozzi, S. Santucci, and P. Picozzi, Phys. Rev. B **48**, 13 430 (1993); A. Di Cicco, M. De Crescenzi, R. Bernardini, and G. Mancini, Phys. Rev. B **49**, 2226 (1994); A. Filipponi, M. Passacantando, L. Lozzi, S. Santucci, P. Picozzi, and A. Di Cicco, Solid State Commun. **91**, 555 (1994).
[9] I. Arčon, A. Kodre, M. Štuhec, D. Glavič-Cindro, and W. Drube, Phys. Rev. A **51**, 147 (1995).
[10] A. Filipponi, E. Bernieri, and S. Mobilio, Phys. Rev. B **38**, 3298 (1988).
[11] P. D'Angelo, A. Di Cicco, A. Filipponi, and N. V. Pavel, Phys. Rev. A **47**, 2055 (1993).
[12] G. Li, F. Bridges, and G. S. Brown, Phys. Rev. Lett. **68**, 1609 (1992); E. Burattini, P. D'Angelo, A. Di Cicco, A. Filipponi, and N. V. Pavel, J. Phys. Chem. **97**, 5486 (1993); M. Takahashi, S. Emura, K. Omote, S. Yoshikado, Y. Ito, N. Takahashi, and T. Mukoyama, Bull. Inst. Chem. Res. (Kyoto) **71**, 37 (1993); A. Filipponi, Physica B **208 & 209**, 29 (1995).
[13] A. Di Cicco and A. Filipponi, Phys. Rev. B **49**, 12 564 (1994).
[14] A. Filipponi and A. Di Cicco, Nucl. Instrum. Methods Phys. Res. Sect. B **93**, 302 (1994).
[15] J. A. Bearden and A. F. Burr, Rev. Mod. Phys. **39**, 125 (1967).
[16] Y. Ito, T. Mukoyama, S. Emura, M. Takahashi, S. Yoshikado, and K. Omote, Phys. Rev. A **51**, 303 (1995).
[17] J. Desclaux, Comput. Phys. Commun. **9**, 31 (1975); J. Phys. B **4**, 631 (1971).